

A CHAOS-BASED PHASE-CODED OFDM SIGNAL FOR JOINT RADAR-COMMUNICATION SYSTEMS

Jingjing Zhao, Kai Huo, Xiang Li
College of Electronic Science and Engineering
National University of Defense Technology
Changsha Hunan Province, China
xiaosatianyu@163.com

ABSTRACT

In this paper, a phase-coded OFDM signal based on chaos theory for joint radar-communication systems is proposed. The signal has high time-frequency product and flexibility in waveform design. A new approach of getting phase codes from chaotic sequences is introduced, and the new codes own good correlation performance. The peak-to-mean envelope power ratio (PMEPR) and the auto-correlation function (ACF) are two important indexes of the signal. PMEPR is decreased to a pretty low level by specific sub-carrier weighing method through systematically research in this paper, while the side-lobe level of ACF of the signal is demonstrated to be relatively low using the sub-carrier complex weight and chaos-based phase code.

Keywords- joint radar-communication system, chaos-based coding, PC-OFDM signal, PMEPR, ACF

1. INTRODUCTION

A Joint radar-communication system uses one platform and waveform to implement the functions of both radar and communication. The key point is to find a sharing signal appropriate for both radar target detection and information transmission. Orthogonal frequency diversity multiplexing (OFDM) signal with high spectrum efficiency and good anti-multipath performance, is widely recognized as the core technique of the 4th generation wireless communication. OFDM radar also gains attention as a new method for range and Doppler estimation because of its big time-bandwidth product. Using OFDM signal, scholars from University of Miami [1] developed a wideband system for both radar and communication. Similar researches were carried out in

German, French, and Dutch [2-5], ONERA, the French Aerospace Lab [2, 3] successfully developed a UWB radar and communication system named HYCAM used for RCS measurement for time-varying targets. Present joint radar and communication systems adopt two major operating modes: time division mode and frequency division mode. In time division structure, radar and communication functions are carried out in different time intervals; while in frequency division structure, different functions are implemented at different sub-carriers.

Phase-coded OFDM signal [6-9], whose sub-carriers are modulated by specific phase sequences, has high flexibility of waveform design by adding more factors, and has better confidentiality performance for communication. However, there are only limited numbers of phase codes with high performance, and most of them are fixed in coding-length, coding-phase number and sequences, thus could be decoded by enemies easily. Chaos-based codes avoid those drawbacks. Discrete-time chaotic signals are pseudorandom sequences sharing lots of properties with random sequences[10-13], and have some unique properties. Different from noise, chaotic signal is determined only by its initial state and free parameters, thus could be duplicated and decoded. Through quantization coding, we get phase codes suitable for radar and communication from chaotic sequences in Part 2, which has relatively good aperiodic correlation property.

In part 3, Peak-to-mean envelope power ratio (PMEPR) and auto correlation function (ACF) are analyzed. Due to its structure, one major drawback of OFDM signal is its varying amplitude, which operates the power amplifier in electron system at a large input backoff. PMEPR measures the fluctuation extent of signal envelope. To ease the problem of high PMEPR brings to system, three major ways are taken:

amplitude limit through before processing, tolerance improvement of the devices, and structure change through sub-carrier weighting. The first method would cause information loss and ruin of the sub-carrier orthogonality, while the second one would increase the system complexity and cost, thus the third one is adopted in this paper. ACF of the signal determines radar range-resolution and communication quality in anti-noise aspects. The ideal ACF has single peak value and low side-lobe ACF. Due to the ideal correlation property of chaotic sequence, chaos-based PC-OFDM signal has relatively acceptable ACF performance, which is demonstrated in this paper.

2. CHAOS-BASED PC-OFDM SIGNAL GENERATION

2.1. Chaos Definition and Characteristics

Chaos, a unique state of nonlinear dynamic system [11], owns some special features, including sensitivity to initial state, ergodicity property, pseudo-randomness property, long-term unpredictability, and ideal correlation property. Table 1 lists the iterative algorithms and free parameters of three common used chaotic systems:

Table 1. Chaos iterative equations and free parameters

Map	Iterative algorithm	Free parameter
Bernoulli	$x_{k+1} = \begin{cases} bx_k + 0.5, & x_k < 0 \\ bx_k - 0.5, & x_k \geq 0 \end{cases}$	b
Logistic	$x_{n+1} = 1 - \lambda x_n^2$	λ
Tent	$x_{n+1} = \alpha - 1 - \alpha x_n $	α

Chaotic signals appear noise like and also share lots of properties with white noise, yet they are all derived by simple nonlinear iterative map equations. A chaotic system is decided only by its initial state x_0 and free parameters. Its initial state sensitivity could be described as: a slight change in initial state x_0 would cause a thorough change in its sequence, which brings its unique performance of confidentiality for communication. Chaotic signal has impulse shape auto-correlation function and cross-correlation function closing to zero, realizing high resolution radar imaging and high quality communication.

2.2. Chaos-based code procedure and PC-OFDM signal

There are large quantities of chaotic sequences, and based on chaos theory, the following quantization coding formula is proposed for getting poly-phase codes:

$$\sigma_k = \text{ceil}\left[N_p(x'_k + 0.5)\right] / N_p * 2\pi \quad (1)$$

With $\{x'_k \mid k = 0, 1, \dots, K-1\}$ being the K -length sequence cut from initial chaotic sequence constrained in $[-0.5, 0.5]$, and N_p being the number of code phases. For Logistic and Tent chaos whose constrained domain is $[-1, 1]$, the sequence would be firstly transformed into $[-0.5, 0.5]$ through dividing every single bit by 2, and (1) goes to:

$$\sigma_k = \text{ceil}\left[N_p(x'_k / 2 + 0.5)\right] / N_p * 2\pi \quad (2)$$

The procedure of getting chaos-based codes is described in Fig. 1

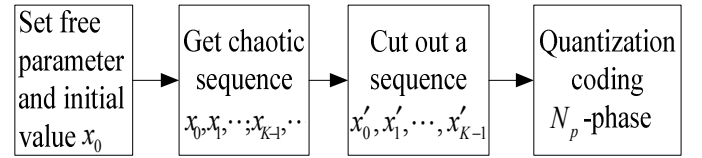
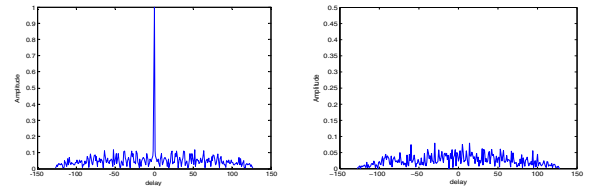


Fig. 1. Flow diagram for getting N_p -phase chaos-based code

Aperiodic auto and cross-correlation function of a 4-phases 128-bits code gotten from Logistic chaotic sequence is shown in Fig. 2. Peak-to-side-lobe ratio (PSLR) in (a) is 18.4520, and the cross-correlation function is near to zero at every time index. Chaos-based phase-codes own relatively good aperiodic correlation property, easy method to generate and flexible code-length and code-phases.



(a) Auto-correlation function (b) Cross-correlation function

Fig. 2. Aperiodic auto and cross-correlation property of 4-phases 128-bits Logistic chaos-based code

Phase-coded OFDM was firstly introduced by Levanon and Mozeson [6, 9], every single pulse consists of N phase-coded sequences transmitted simultaneously on N sub-carriers. Each sequence contains K bits. Expression of PC-OFDM pulse complex envelope is :

$$s(t) = \sum_{n=0}^{N-1} \sum_{k=0}^{K-1} w_n a_{n,k} \text{rect}\left[\frac{t - kt_b - 0.5t_b}{t_b}\right] \exp(j2\pi n \Delta f t) \quad (3)$$

$$= \sum_{n=0}^{N-1} w_n u_n(t) \exp(j2\pi n \Delta f t)$$

In which, w_n is the complex weight of the n th sub-carrier, $a_{n,k}$ is k th code on the n th sub-carrier, t_b is the bit duration, $T=Kt_b$ is the pulse length, and Δf is the frequency interval of the adjacent two sub-carriers. To meet the orthogonal condition, Δf has to be:

$$\Delta f = 1/t_b \quad (4)$$

Thus the bandwidth of the PC-OFDM signal is:

$$B = N\Delta f = N/t_b \quad (5)$$

The time-frequency product equals to MN , which is relatively large comparing to traditional radar signal.

With the chaos-based code $\{\sigma_k | k=0,1,\dots,K-1\}$ got before, $a_{n,k}$ in (3) is defined as:

$$a_{n,k} = e^{j\sigma_{n,k}} \quad (6)$$

According to the code sequence, there are two types of OFDM signal. IS PC-OFDM uses identical sequence to modulate all sub-carriers, where $a_{n,k}=a_k$ for all $n=1,2,\dots,N-1$; NIS one uses different sequence to modulate different sub-carriers. IS PC-OFDM keeps good orthogonality between sub-carriers and is terse in signal form for the further processing such as decoding, while NIS one carries more information, has relatively better correlation property. In this paper, IS signal is mainly discussed.

3. PMEPR AND ACF OF IS PC-OFDM SIGNAL

For IS PC-OFDM signal, the complex envelope is defined as:

$$s(t) = \sum_{k=0}^{K-1} a_k \text{rect}\left[\frac{t - kt_b - 0.5t_b}{t_b}\right] \sum_{n=0}^{N-1} w_n \exp(j2\pi n \Delta f t) \quad (7)$$

$$= \sum_{k=0}^{K-1} v_k(t) \text{rect}\left[\frac{t - kt_b - 0.5t_b}{t_b}\right]$$

$$= u(t) \sum_{n=0}^{N-1} w_n \exp\left(j2\pi n \frac{t}{t_b}\right)$$

Complex envelope of the k th multi-carrier bit is:

$$v_k(t) = a_k \sum_{n=0}^{N-1} w_n \exp\left(j2\pi n \frac{t}{t_b}\right) \quad (8)$$

And complex envelope of each sub-carrier is:

$$u(t) = \sum_{k=0}^{K-1} a_k \text{rect}\left(\frac{t - kt_b - 0.5t_b}{t_b}\right) \quad (9)$$

In this section, PMEPR and ACF of IS PC-OFDM signal are studied, we firstly optimize PMEPR through complex weighting, and secondly deduce mathematical expression of ACF and find the influencing factors.

3.1. PMEPR

Peak-to-Mean envelope power ratio (PMEPR) is defined as:

$$PMEPR = \frac{P_{peak}}{P_{mean}} = \frac{\left[\max_{t \in [0,T]} \{|s(t)|\} \right]^2}{(1/T) \int_0^T |s(t)|^2 dt} \quad (10)$$

2 is the common upper limit of PMEPR to avoid saturations or other nonlinearity of the electron systems, while the PMEPR is equal to N if and only if all subcarriers are of equal energy (uniformly weighted). Due to $|a_k|=1$, each bit shares the same complex envelope, thus the problem of decreasing the PMEPR of the signal comes to the problem of decreasing the PMEPR of a single bit, and the PMEPR is lowered by proper amplitude and phase weighting of various sub-carriers only, but unrelated to phase coding length and sequence. A 128-bit 4-phase Logistic chaos-based code is used in the following analysis to modulate all the sub-carriers.

Table 2 Lists three amplitude windows used for PMEPR decreasing along with the rectangular window, in which, $n=0,1,2,\dots,N-1$.

Table 2. Amplitude window definition

Amplitude window	Definition
Rectangular	$ w_n =1$
Hanning	$ w_n = \left[0.54 - 0.46 \cos \frac{2\pi n}{N} \right]^{0.5}$
Hamming	$ w_n = \left[0.5 - 0.5 \cos \frac{2\pi n}{N} \right]^{0.5}$
Blackman	$ w_n = 0.42 - 0.5 \cos \frac{2\pi n}{N} + 0.08 \cos \frac{4\pi n}{N}$

To simplify the discussion, $\{w_n\}$ is normalized that $\sum_{n=0}^{N-1} |w_n|^2 = 1$, to make $P_{mean}=1$.

Fig. 3 depicts the PMEPRs of four multicarrier bits weighted with the four amplitude windows above as a function of number of sub-carriers N . Amplitude window does not change the envelope shape of the bit, but just compresses the fluctuation between peaks. PMEPR grows almost linearly with N for all the four windows in Fig. 3, Blackman window performs relatively best but cannot control it under 2 for $N > 2$.

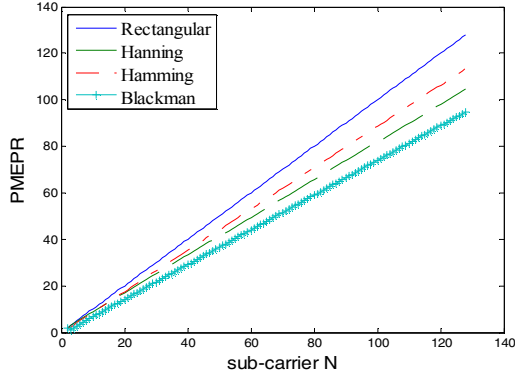


Fig. 3. PMEPR varying with sub-carrier number N , amplitude window with none initial phase

Three common used initial phases are listed in Table 3, in which, $n = 0, 1, 2, \dots, N-1$.

Table 3. Initial phase definition

Initial phase	Definition
Newman	$\theta_n = \frac{n^2}{N} \pi$
Schroeder	$\theta_n = -2\pi \sum_{l=1}^{n-1} (n-l) w_l ^2 - 2\pi \lambda \frac{n}{N}$
Narahashi- Nojima	$\theta_n = \frac{(n-1)(n-2)}{N-1} \pi$

The curves in Fig. 4 show the performances of the three initial phases combined with rectangular window. PMEPRs decrease slightly with N for all of them, and for $N > 6$, PMEPRs are all under 2. With rectangular window, Newman and Schroeder phases are equivalent to each other, excelling Narahashi-Nojima phases slightly in performance for larger N s. While For Newman and Schroeder phases, the PMEPRs are relatively lower at even N s than at odd ones.

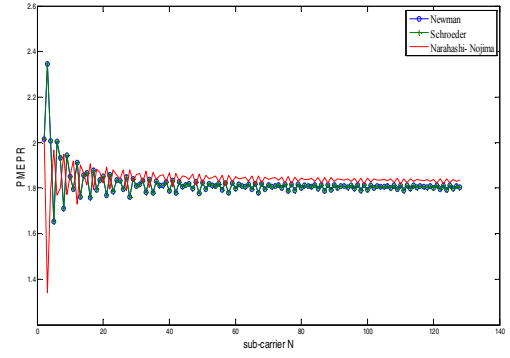


Fig. 4. PMEPR varying with sub-carrier number N , initial phase with rectangular window

Combined weighting methods are discussed in Fig. 5-Fig. 7, in which the PMEPR decreasing performances of 12 combined weighting schemes are depicted. In each picture, one phasing approach is combined with 4 amplitude windows, PMEPRs are compared as a function N .

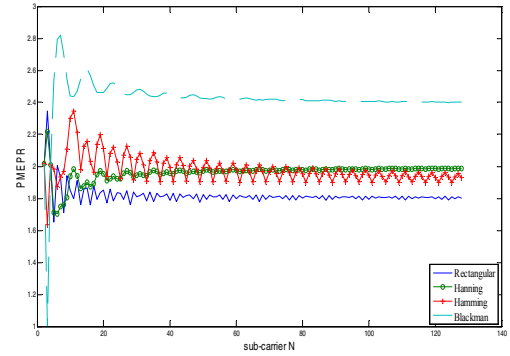


Fig. 5. PMEPR, Newman phases combined with amplitude windows

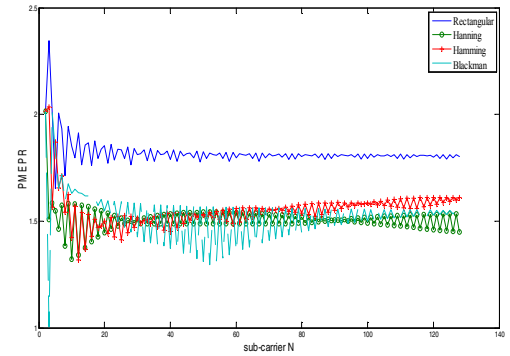


Fig. 6. PMEPR, Schroeder phases combined with amplitude windows

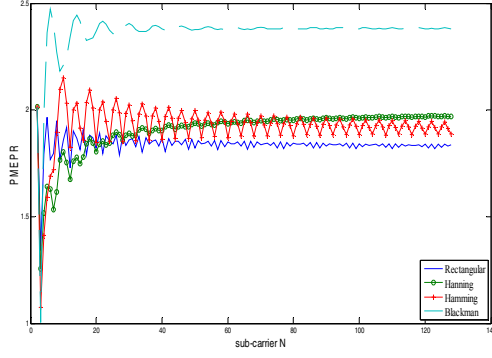


Fig. 7. PMEPR, Narahashi- Nojima initial phase combined with amplitude windows

As shown in Fig. 5 and Fig. 7, for Newman and Narahashi-Nojima phases, once combined with three windows rather than the square window, PMEPR will increase especially for Blackman window. But for Schroeder phases, due to the coupling relationship between Schroeder phases and sub-carrier amplitudes, values of PMEPR are depressed to a large extent, as can be seen in Fig. 6. Blackman window performances best at even N s; while for larger N s, the difference between Hanning window and Blackman window becomes smaller; and for $N > 100$, Hanning window combined with Schroeder has highest performance.

3.2. Auto-correlation function

Complex envelope of each sub-carrier $u(t)$ is a Phase-coded pulse, whose ACF is:

$$R_{uu}(\tau) = \int_{-\infty}^{\infty} \sum_{m=0}^{K-1} a_m \text{rect}\left(\frac{t - mt_b}{t_b}\right) \sum_{n=0}^{K-1} a_n \text{rect}\left(\frac{t - nt_b + \tau}{t_b}\right) dt \quad (11)$$

$$\stackrel{\tau = it_b + \eta}{=} (t_b - \eta) R_a[i] + \eta R_a[i+1]$$

Thus ACF of $s(t)$ can be written as:

$$R_{ss}(\tau) = \sum_{n=0}^{N-1} \sum_{l=0}^{N-1} w_n w_l^* \int_{-\infty}^{\infty} u(t) u^*(t + \tau) \cdot \exp\left(j2\pi n \frac{t}{t_b}\right) \exp\left(-j2\pi l \frac{t + \tau}{t_b}\right) dt \quad (12)$$

$$\stackrel{\tau = it_b + \eta}{=} \sum_{n=0}^{N-1} \sum_{l=0}^{N-1} w_n w_l^* \exp\left(-j2\pi l \frac{\eta}{t_b}\right) \cdot \{I_1 R_a[i] + I_2 R_a[i+1]\}$$

Where

$$I_1 = (t_b - \eta) \text{sinc}\left(\pi(n-l) \frac{t_b - \eta}{t_b}\right) \exp\left(j\pi(n-l) \frac{\eta}{t_b}\right),$$

$$I_2 = \eta \text{sinc}\left(\pi(n-l) \frac{\eta}{t_b}\right) \exp\left(j\pi(n-l) \frac{\eta}{t_b}\right)$$

ACF is a function of both the complex sub-carrier weights $\{w_n\}$ and the phase coding sequence $\{a_k\}$.

At integer multiples of the bit duration t_b , where $\eta = 0$, yielding:

$$R_{ss}(it_b) = t_b R_a[i] \sum_{n=0}^{N-1} |w_n|^2 = t_b R_a[i] \quad (13)$$

Denoting that it is determined only by the aperiodic auto-correlation of the coding sequence $\{a_k\}$ and coding length K . K can be increased to help improve ACF, but cannot grow without limitation because it also increase signal complexity and pulse length. Chaos-based phase codes with good correlation property are adopted here to compress the side-lobes at integer multiples of t_b , while ACFs inside the coding bits are compressed by sub-carrier weighting proposed before.

Fig. 8 compares ACF of a 32-sub-carrier IS PC-OFDM signal and a single-carrier PC signal. They are modulated by the same 128-bit 4-phase Logistic chaos-based code. For OFDM signal, sub-carriers are weighted with Hanning window and Schroeder initial phase. For better observation, ACF within 0 to $20t_b$ is shown in the figure. At integer multiples of the bit duration t_b , the values are equal to each other and are close to 0.1 (normalized), demonstrating that N has nothing to do with ACF at those moments. While inside the coding bits, ACFs of OFDM signal are nearly zero except for the first bit.

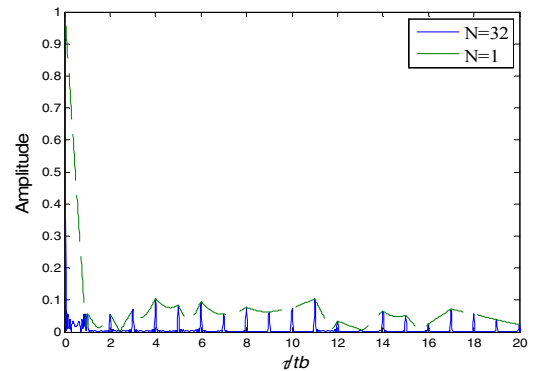


Fig. 8. ACF of a Logistic-based 128-bit 4-phase coded 32-sub-carrier OFDM signal weighted with Hanning window and Schroeder initial phase

4. CONCLUSION

Joint radar and communication application calls for an appropriate sharing signal waveform to implement both radar and communication functions. Phase-coded OFDM signal, with high time and frequency product and spectrum efficiency, possesses both high range-Doppler resolution in radar field and the ability of anti-multipath and anti-inter-symbol interference in communication field. Using chaotic sequences, a phase codes generating procedure is proposed in this paper. Chaos-based phase codes have several good properties including the ease of their generation, their flexibility in coding length and coding phase number, unique secrecy performance due to their sensitive dependence on initial condition, and their ideal correlation properties, so they are suitable for PC-OFDM signal modulation.

In this paper, PMEPR and ACF of IS PC-OFDM signal are analyzed mainly. For IS signal, PMEPR is influenced only by sub-carrier complex weights. PMEPR is analyzed as a function of both sub-carrier number N and weighting methods, and the conclusion that Hanning window combined with Schroeder phases performances best for larger sub-carrier number N is finally. Also, mathematical expression of the ACF is deduced. At integer multiples of the bit duration t_b it is determined only by the aperiodic auto-correlation of the coding sequence $\{a_k\}$ and coding length K ; while inside the bits, it is also influenced by sub-carrier weighting. A 32-sub-carrier IS-OFDM signal coded with a 128-bit Logistic-chaos based phase code and weighted with Hanning window and Schroeder phases has relatively acceptable ACF with the highest side-lobe being 0.1 and values inside the coding bit close to zero except for the first bit.

To better implement the communication function of the system, waveform design and property analysis of NIS PC-OFDM signal would be in the further research. Researches about how to add transmitted information into the modulated phases, and how to assure technical indicator of $\text{PMEPR} < 2$ and further compress the side-lobe of ACF in NIS structure based on chaos theory would be carried out later.

5. ACKNOWLEDGEMENT

Thanks to the foundation of the State Key Laboratory CEMEE (CEMEE2014K0207B) and the foundation of China Aerospace Science and Technology Corporation (CASC) for funding.

REFERENCES:

- [1] D. Garmatyuk, J. Schuerger, K. Kauffman, and S. Spalding, "Wideband OFDM system for radar and communications," in *IEEE National Radar Conference - Proceedings*, Pasadena, CA, United States, 2009.
- [2] Y. Paichard, "Orthogonal multicarrier phased coded signal for netted radar systems," in *2009 International Waveform Diversity and Design Conference Proceedings, WDD 2009*, Kissimmee, FL, United States, 2009, pp. 234 - 236.
- [3] Y. Paichard, J. C. Castelli, P. Dreuillet, and G. Bobillot, "HYCAM: a RCS measurement and analysis system for time-varying targets," in *Instrumentation and Measurement Technology Conference*, Sorrento, Italy, 2006, pp. 921-925.
- [4] C. Sturm, T. Zwick and W. Wiesbeck, "An OFDM system concept for joint radar and communications operations," in *IEEE Vehicular Technology Conference*, Barcelona, Spain, 2009, pp. 1-5.
- [5] G. Lellouch and H. Nikookar, "On the capability of a radar network to support communications," in *14th IEEE Symposium on Communications and Vehicular Technology in the Benelux*, Delft, 2007, pp. 1-5.
- [6] N. Levanon, "Multifrequency complementary phase-coded radar signal," *IEE Proc.-Radar, Sonar Navigation*, vol. 147, pp. 276-284, 2000.
- [7] N. Levanon, "Multicarrier radar signal - pulse train and CW," *IEEE Trans. AES*, vol. 38, pp. 707-720, 2002.
- [8] N. Levanon, "Multicarrier radar signals with low peak-to-mean envelope power ratio," *IEE Proc. Radar Sonar and Navigation*, vol. 150, pp. 71-77, 2003.
- [9] N. Levanon and E. Mozeson, *Radar Signals*. New York: John Wiley & Sons, Inc., Hoboken, 2004.
- [10] E. M. El-Bakary, O. Zahran, S. A. El-Dolil, and F. E. A. El-Samie, "Chaotic Maps: A Tool to Enhance the Performance of OFDM Systems," *International Journal of Communication Networks and Information Security*, pp. 54-58, 2009.
- [11] S. Harman, "The Diversity of Chaotic Waveforms in Use and Characteristics," 2010.
- [12] M. Hilmey, S. Elhalafwy and M. Z. Eldin, "Efficient transmission of chaotic and AES encrypted images with OFDM over an AWGN channel," pp. 353-358, 2009.
- [13] B. Pan, J. Feng, Q. Li, and Q. Tao, "Image communication system based on chaotic FH-OFDM technique," pp. 546-550, 2010.